

Surface modification of a DNA tetrahedron

Chuan Zhang[†], Min Su[‡], Yu He[†], Yujun Leng[‡], Alexander E. Ribbe[†], Guansong Wang[±], Wen Jiang[†] & Chengde Mao^{†*}

[†]*Department of Chemistry, [‡]Markey Center for Structural Biology and Department of Biological Sciences, Purdue University, West Lafayette, Indiana 47907, USA; [±]Institute of Respiratory Diseases, Xinqiao Hospital, The Third Military Medical University, Chongqing, China.*

Supplementary Information

Materials and Methods

Oligonucleotides. DNA sequences were adapted from previous works, which were originally designed by a computer program “SEQUIN” (Seeman, N. C. *J. Biomol. Struct. Dyn.* **1990**, *8*, 573-581). All oligonucleotides were purchased from IDT, Inc. and purified by 15-20% denaturing polyacrylamide gel electrophoresis (PAGE). DNA sequences: central long strand **L** (blue-red): Agg CAC CAT CgT Agg TTT TCT TgC CAG gCA CCA TCg TAG gTT TTC TTg CCA ggC ACC ATC gTA ggT TTT CTT gCC; medium strand **M** (green and purple): TAg CAA CCT gCC TgA gCg CTT TTg CgC TgT gCA AgC CTA CgA Tgg ACA Cgg TAA TgA C; short peripheral strand **S** (black): TTA Ccg TgT ggT TgC TAG gCg.

Formation of DNA complexes. DNA strands were combined according a molecular ratio of **L:M:S** = 1:3:3 in Tris-Acetic-EDTA-Mg²⁺ (TAE/Mg²⁺) buffer. The DNA solution was slowly cooled down from 95 °C to 25 °C over 24 hours. TAE/Mg²⁺ buffer contained 40 mM Tris base (pH 8.0), 20 mM acetic acid, 2 mM EDTA and 12.5 mM magnesium acetate.

Non-denaturing PAGE. Gels contained 4% polyacrylamide (19:1 acrylamide/bisacrylamide) and were run on a FB-VE10-1 electrophoresis unit (FisherBiotech) at 4°C (100 V, constant voltage). The running buffer was TAE/Mg²⁺ buffer. After electrophoresis, the gels were stained with Stains-All (Sigma) and scanned.

Atomic Force Microscope Imaging. A drop of 2 μL DNA solution was spotted onto freshly cleaved mica surface, and kept for 10 seconds to achieve strong adsorption. The sample drop was then washed off by 30 μL 2 mM magnesium acetate solution, and dried by compressed air. DNA samples were imaged by tapping-mode AFM on Nanoscope IIIa (Digital Instruments) with NSC15 tips (silicon cantilever, MikroMasch). The tip-surface interaction was minimized by optimizing the scan set-point.

Dynamic Light Scattering. 15 μL sample solution (after complex formation) was directly measured by DynaPro 99 (Protein Solutions) with a laser (wavelength: 826.3 nm).

Cryogenic Transmission Electron Microscope Imaging. After formation, DNA hairpin-tetrahedron solutions were concentrated to ~10 μM with Microcon YM-100 (100 kDa) Centrifugal Filter Units. A drop of 3 μl concentrated DNA solution was pipetted onto a Quantifoil grid. Then, the grid was blotted and immediately plunge-frozen into ethane slush cooled by liquid nitrogen. The images were taken under low-dose condition to minimize radiation damages to the samples. To enhance the image contrast, under-foci in the range of 2–4 μm were used to record the images. The calibrated magnification used for DNA hairpin-tetrahedron was ×52,260, resulting in pixel sizes of 2.20Å.

Single-particle reconstruction. 3D reconstructions of the DNA hairpin-tetrahedron used the single-particle image processing software EMAN [Ludtke, S. J., Baldwin, P. R. & Chiu, W. EMAN: Semiautomated software for high-resolution single-particle reconstructions. *J. Struct. Biol.* **128**, 82–97 (1999)]. The initial model was built using 100 randomly selected raw particles. The initial orientations of individual particles were randomly assigned within the corresponding asymmetry unit of the tetrahedron.

2599 particles were used for the single-particle reconstruction. 239 reference projections in the tetrahedron asymmetric unit were generated with an angular interval of 2.5°. A projection matching algorithm was then used to determine the centre and orientation of raw particles in the iterative refinement. The tetrahedron symmetry was imposed during the reconstruction. The map resolution was determined to be at 2.6 nm using the Fourier shell correlation (0.5 threshold criterion) of two 3D maps independently built from half data sets. Control reconstructions with lower symmetries imposed were performed to check that particles indeed have tetrahedron symmetry. Final 3D maps were visualized using UCSF Chimera software [Goddard, T. D., Huang, C. C. & Ferrin, T. E. Visualizing density maps with UCSF chimera. *J. Struct. Biol.* **157**, 281–287 (2007)].

Figure S1. PAGE gel analysis of the impact of the central single-stranded loop length on the DNA hairpin-tetrahedron formation. The tetrahedron ladder prepared by a ratio of 1:3:1.5 (L:M:S). In such condition, dimer, trimer, tetramer can form at the same time. The shorter the central loops are, the more rigid the motif is. 4T-loops provide the correct the 3-point-star tiles with proper flexibility to form the tetrahedron with hairpins.

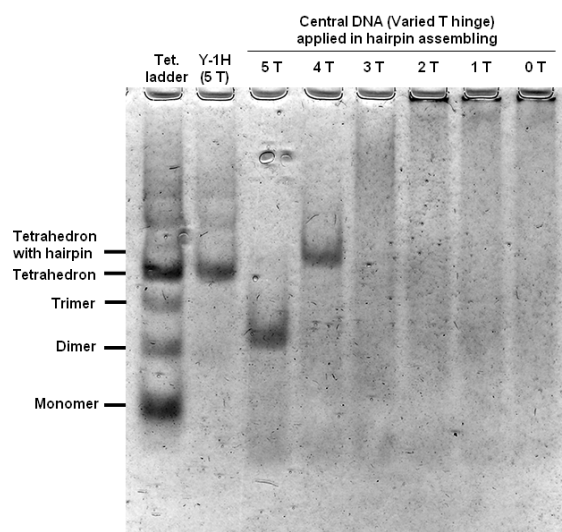


Figure S2. Characterization of the DNA tetrahedron with hairpins by dynamic light scattering (DLS) and atomic force microscopy (AFM). (a) DLS shows the size histogram of DNA tetrahedron with hairpins; (b) An AFM image of DNA hairpin-tetrahedra and a close-up view (inset).

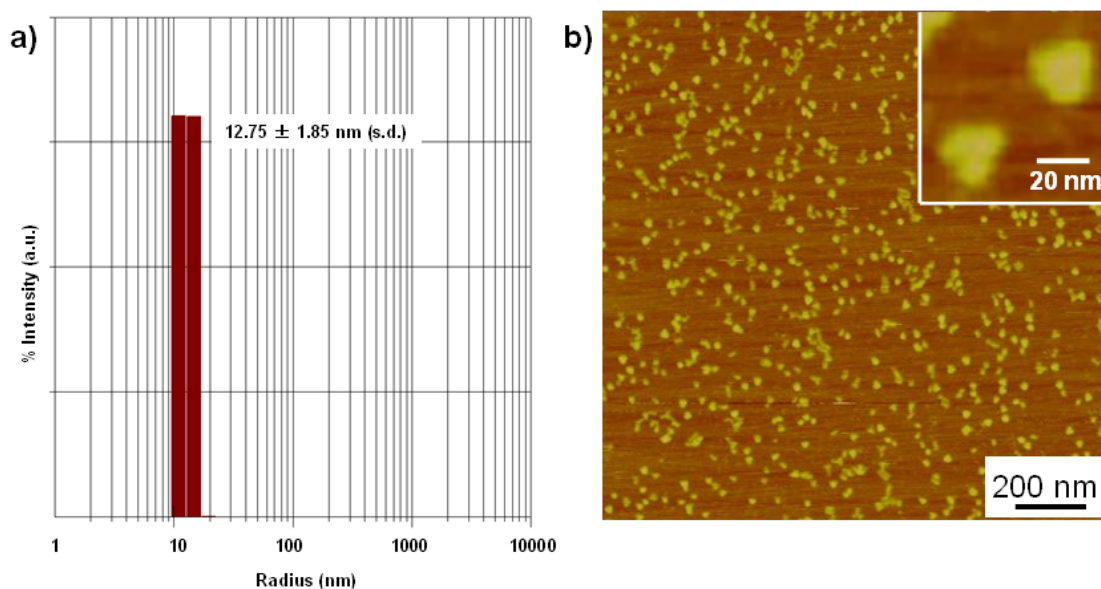


Figure S3. Three views of the DNA tetrahedron with hairpin structures reconstructed by relaxing to lower C3 symmetry.



Figure S4. A DNA hairpin-tetrahedron: its class averaged images (top row) and the corresponding projections (bottom row) from the structural model. 80 of total 239 pairs of class averaged images and projections were selected to show with interval step of 3.

